NRL Memorandum Report 3283

Microwave Radiometric Detection of Atmospheric Internal Waves

LEE U. MARTIN AND CHARLES I. BEARD

Airborne Radar Branch
Radar Division

May 1976

NAVAL RESEARCH LABORATORY
Washington, D.C.

SECURITY CLASSIFICATION OF THIS PAGE (When Data Entered)

REPORT DOCUMENTATION PAGE

READ INSTRUCTIONS BEFORE COMPLETING FORM

1 REPORT NUMBER: NRL Memorandum Report 3283	2 GOVT ACCESSION NO.
3 RECIPIENT'S CATALOG NUMBER	
4 TITLE (and Subtitle): MICROWAVE RADIOMETRIC DETECTION OF ATMOSPHERIC INTERNAL WAVES	5 TYPE OF REPORT & PERIOD COVERED: Interim report on a continuing NRL problem.
	6 PERFORMING ORG. REPORT NUMBER
7 AUTHOR(s): Lee U. Martin and Charles I. Beard	8 CONTRACT OR GRANT NUMBER(s)
9 PERFORMING ORGANIZATION NAME AND ADDRESS: Naval Research Laboratory, Washington, D.C. 20375	10 PROGRAM ELEMENT, PROJECT, TASK AREA & WORK UNIT NUMBERS: NRL Problem R07-37; Project RR 021-01-41, 61153N21
11 CONTROLLING OFFICE NAME AND ADDRESS: Department of the Navy, Office of Naval Research, Arlington, Virginia 22217	12 REPORT DATE: May 1976
	13 NUMBER OF PAGES: 31
14 MONITORING AGENCY NAME & ADDRESS (if different from Controlling Office)	15 SECURITY CLASS. (of this report): UNCLASSIFIED
	15a DECLASSIFICATION/DOWNGRADING SCHEDULE

16 DISTRIBUTION STATEMENT (of this Report)

Approved for public release; distribution unlimited.

16 NRL-R07-37
RR021-01

17 DISTRIBUTION STATEMENT (of the abstract entered in Block 20, if different from Report)

17 RR021-01-41

18 SUPPLEMENTARY NOTES

19 KEY WORDS (Continue on reverse side if necessary and identify by block number)

Microwave radiometry
Atmospheric internal waves
Remote sensing
Atmospheric layers

20 ABSTRACT (Continue on reverse side if necessary and identify by block number)

Microwave radiometers have, for the first time, detected internal waves in the atmospheric boundary layer and localized their altitude. Varying the intersection height of a narrow (3°) antenna beam with that of a wide (22°) vertically pointing antenna beam allowed determination of the wave altitudes.

The ground-based radiometers were located at San Diego, where, in an experiment in May-June 1975, the Naval Electronics Laboratory Center (NELC) provided "atmospheric-truth" for

(Continues)

DD FORM 1 JAN 73 1473 EDITION OF 1 NOV 65 IS OBSOLETE
S/N 0102-014-6601

SECURITY CLASSIFICATION OF THIS PAGE (When Data Entered)

20. Abstract (Continued)

comparison to the radiometer data obtained by the Naval Research Laboratory. NELC provided FM-CW radar, acoustic sounder, lidar, microbarograph, radiosonde, and surface meterological data.

Preliminary results showed cases of correspondence between the signals of the passive radiometers and the active FM-CW radar and acoustic sounder systems. Examples included internal wave trains up to an hour in length.

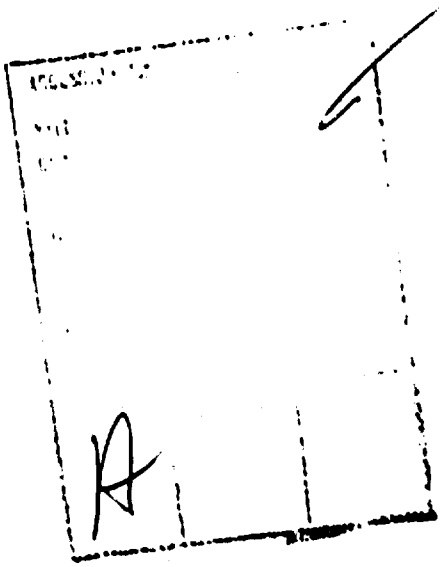

CONTENTS

MEMORANDUM

Subj: Microwave Radiometric Detection of Atmospheric Internal Waves

BACKGROUND

Atmospheric inversion layers and associated internal waves may cause ducting conditions and radar holes which adversely affect the performance of Navy radars and communications. A ground-based passive method of detecting internal waves associated with inversion layers would be useful to the Navy, particularly during times of radio silence. An experiment was therefore conducted to determine whether internal waves could be detected with microwave radiometers and localized in altitude. The ground-based radiometers were located at San Diego where the Naval Electronics Laboratory Center (NELC) provided "atmospheric-truth" for comparison to the radiometer data obtained by the Naval Research Laboratory. NELC provided FM-CW radar, acoustic sounder, lidar, microbarograph, radiosonde and surface meteorological data for the comparison. This report describes measurements conducted over two separate intervals, 7-23 May and 16-30 June 1975.

FINDINGS

For the first time, microwave radiometers have detected internal waves in the atmospheric boundary layer and have localized their altitude. Varying the intersection height of a narrow (3°) antenna beam with that of a wide (22°) vertically pointing antenna beam allowed determination of the altitude of the waves. Correlation between the two radiometer signals was a maximum when the altitude of the waves corresponded to the height of the beam intersection. Preliminary results showed cases of correspondence between the signals of the passive radiometers and the active FM-CW radar and acoustic sounder systems. Examples included internal wave trains up to an hour in length.

RESEARCH IMPLICATIONS

Analysis of the data has led to devising a possible method to measure the thickness of the inversion layer (Δh) and the index of refraction change across the layer (Δh). These quantities, in addition to layer altitude, would then enable calculation of ray tracing plots to show radar ducting and hole conditions.

RECOMMENDATIONS

The analysis of the data should continue to determine further correspondences and differences between the passive (radiometer) and active (FM-CW radar and acoustic sounder) systems. A second experiment is now in progress to test potential methods of determining the inversion layer thickness and the index of refraction change (ΔN), which no other remote sensor can do.

MICROWAVE RADIOMETRIC DETECTION OF ATMOSPHERIC INTERNAL WAVES

1. INTRODUCTION

Internal waves have become an important phenomenon to atmospheric physics, meterology, and electromagnetic propagation. Internal wave motion is now known (Gossard and Hooke, 1975) to be an important factor in the fluid dynamics and meteorology of the atmospheric boundary layer. The wave motion transports momentum and affects atmospheric circulation. One type of shear induced wave motion (Kelvin-Helmholtz) can become unstable, break down, and generate turbulence. Conversely, turbulence, as well as other sudden disturbances, can initiate internal waves on density interfaces within the atmosphere.

Interaction of electromagnetic (EM) waves with the internal waves can be a problem or not, depending upon the application. EM waves emanating from a transmitter at low elevation angles can encounter a convergence, or steepening, of the index of refraction gradient in the inversion layer caused by waves on the layer; the result can be a so-called radio "hole", or loss of signal (Vickers and Lopez, 1975). Useful interaction has been obtained in the last several years with ground-based, upward-looking, active radar (Richter, 1969) or acoustic (McAllister, 1968) remote sensors; the EM (or acoustic) radiation emitted is back scattered from small scale turbulence (of a scale one-half the sensor wavelength).

In this report, we describe the first known detection of atmospheric internal waves by upward-looking, passive microwave radiometers. A 22-GHz radiometer operates on a different principle from the active sensors in that it detects radiation from the vertical distribution of water vapor (primarily); the change in this distribution by the internal wave causes corresponding changes in the radiometer output. The radiometric remote sensor is thus independent of other sensors in that it measures different parameters of the atmosphere and does not require wind shear (to produce turbulence) for detectability of internal waves. The internal waves were detected and localized in altitude during an experiment which was conducted by NRL at the Naval Electronics Laboratory Center (NELC) in the spring of 1975. A semi-permanent low level inversion over southern California separates cool, moist surface air from warm, dry air aloft. This situation is ideal for the propagation of internal waves, a subject of numerous investigations by NELC with FM-CW radars (Gossard, et al., 1970, 1971).

For the experiment, NELC provided "atmospheric truth" in the form of FM-CW radar, acoustic sounder, lidar, radiosondes, microbarograph, and surface meteorological data. Measurements were conducted over two separate intervals, 7-23 May and 16-30 June 1975.

Section 2 describes the atmospheric model and the results of theoretical calculations of the radiometer signal expected from internal waves. Section 3 describes the equipment used in the experiment by both NRL and NELC and Section 4 discusses the experimental setup and procedures. Some preliminary results from both May and June are discussed in Section 5 and some conclusions are presented in Section 6.

Note: Manuscript submitted April 21, 1976.

2. ATMOSPHERIC MODELING

The detection of internal waves with microwave radiometers depends upon temporal variations of water vapor or temperature. These variations can either be changes in magnitude at a specific altitude, or changes in the distribution with height. Prior to the experiment, the sensitivity of a microwave radiometer to variations in the magnitude and distribution of temperature and water vapor in its field of view was calculated on a digital computer. This sensitivity was determined as a function of radiometer frequency, height of the changes, and moisture content of the atmosphere. This section describes the computer model of the atmosphere, the results which were obtained, and a brief investigation of possible changes in brightness temperature caused by the sky background.

2.1 Computer Program

The computer program used in this study is an expansion of a 14-layer model originally developed by Kreiss (1968). The expanded program divides the atmosphere into 202 layers, each five millibars (mb) in thickness. This small layer thickness (equivalent to ≈ 40 meters near the earth's surface) provides relatively fine resolution of temperature and water vapor features. Using standard temperature and water vapor profiles, the program calculates the transmission and resultant emission for each layer using the equations for water vapor and oxygen absorption. Then, the contribution of each layer is appropriately summed to determine the total atmospheric brightness temperature. These computations can be made for any choice of frequency between 1 and 100 GHz. To determine the change in brightness temperature due to either small changes in water vapor or temperature, both the 22.2 GHz water vapor line and the oxygen line near 60 GHz were investigated. In addition, the standard atmospheric temperature and water vapor profiles were modified to reflect the special conditions under which internal waves propagate in the lower atmosphere. These conditions and the atmospheric model are discussed in the following section.

2.2 Atmospheric Model

Earlier work by Gossard (1954), Atlas et al, (1970a) and Richter (1969), has shown that internal wave activity is associated with stable layers (inversions) and with sharp gradients of refractive index. Since the largest changes in refractive index are those due to humidity changes, internal waves will likely occur at the transition region between a cool, moist surface layer with a warm, dry layer above. These conditions are incorporated in a simple two-layer model of the atmosphere which closely resembles the actual conditions observed at San Diego. The moist layer of the model extends from the surface to approximately 0.5 km, separated from the dry layer above by a transition region 40 to 100 meters thick. Within the transition region the temperature increases and the moisture decreases with elevation, resulting in a sharp gradient of refractive index. It is assumed that the internal

waves propagate within or at the boundaries of this transition region, causing both the height and the thickness of the layer to change. These changes will affect the distribution of temperature and water vapor at the lower boundary of the transition region. Results from both types of changes are presented below.

2.3 Results

Preliminary calculations had two primary objectives. The first was to calculate the sensitivity of brightness temperature to water vapor and temperature changes at various observing frequencies. The second was to determine what changes in the profiles of the model would cause changes in brightness temperature of sufficient magnitude to be detectable by a radiometer.

Calculations were made for altitudes of the transition layer of 0.5, 1.0 and 2.0 km and for both standard and humid moisture profiles. A summary of the results is presented below.

A. In the frequency range from 15 to 60 GHz, a microwave radiometer is more sensitive, by an order of magnitude, to fluctuations in water vapor than to fluctuations in temperature. The greatest sensitivity occurs at the 22.235-GHz water vapor line.

B. A change of 0.1°K in brightness temperature will occur for:

(1) a 25% change in water vapor at 0.5 km,
(2) a 20-meter change in the depth of the moist layer, and
(3) a 40-meter change in the thickness of the transition layer, keeping the depth of the moist layer constant.

C. The magnitude of the above changes in brightness temperature will:

(1) decrease with increasing altitude of the transition layer, and
(2) increase with increasing moisture content of the lower atmosphere.

This initial modeling suggested therefore that reasonable changes in either the distribution of water vapor or the amount at a specific height would cause small but measurable changes in the microwave brightness temperature. These changes, although small, would be largest at the water vapor line at 22.2 GHz.

2.4 Background Fluctuations

The relatively small magnitude of the changes in brightness temperature generated by internal waves raises the question of the importance of atmospheric "background noise". The magnitude of this noise, generated by the advection of varying amounts of water vapor through the antenna beam by the wind, depends on atmospheric humidity, size of the air parcels, antenna beamwidth, observing frequency, and radiometer time constant.

To provide an estimate of the noise level, calculations were carried out using the computer program and model described in Section 2.2. The noise sources are assumed to be air parcels whose water vapor content varies by $\pm$ 10% from the environment. These parcels, ranging in diameter from 10 to 100 meters, pass through the antenna beam at altitudes up to 0.5 km with velocities corresponding to a wind speed of 3 m sec^{-1}. The change in brightness temperature, ΔT, caused by these parcels is proportional to the area of the antenna beam filled by the parcel times the temperature difference between the parcel and its environment, or equivalently

$$\Delta T \propto \Delta To \, [D_p/D_b]^2$$

where ΔTo is the brightness temperature difference between the parcel and the environment, and D_p and D_b are the diameters of the parcel and beam respectively. This value for ΔT will be reduced when the parcel is in the antenna beam for a time less than the integration time of the radiometer. For a 3° beamwidth(bw) antenna, changes in brightness temperature as large as those from internal waves can be expected from parcels 100 meters in diameter having humidities $\pm$ 10% different from the local mean. The separation of internal waves from background fluctuations will depend on a cross-correlation analysis of the brightness temperature recordings from the two radiometers or on the sequence of the wave pattern.

3. INSTRUMENTATION

3.1 Microwave Radiometers

The microwave radiometers were identical in design to insure uniform performance and to allow accurate comparisons between them. Figure 1 is a block diagram of a radiometer, and the specifications are listed in Table I.

TABLE I

System Specifications for Dicke Type,
Double Bandwidth Radiometer

Receiver Center Frequency	22.2 GHz
IF Bandwidth	500 MHz
Noise Figure	5 dB
Post Detection Time Constants	0.15, 1.5, 15 Sec
Sensitivity (RMS)	0.28, 0.09, 0.03°K
Antennas	3.3° and 22° beamwidths

To provide for stable measurements over long time periods, the Dicke design was used, switching between the antenna and a reference load immersed in liquid nitrogen. This provides a known and stable reference temperature (T = 77°K) close to the expected sky temperature. A "zero" level was established by having a load identical to the reference load also immersed in the liquid nitrogen. Calibration was performed by injecting a known signal from a solid-state noise source into the system. This calibration could be made either manually or automatically with a timing device. The latter allowed automatic nighttime calibrations when the equipment was left unattended. The output of the synchronous detector was fed to the recorder through a low pass filter with adjustable time constants, two of which, initially, could be recorded simultaneously on the same chart recorder. This was later changed so that the outputs of the two separated radiometers could be recorded simultaneously on the same recorder.

The antenna sizes were chosen to provide spatial resolution of the shortest internal waves expected and to allow localization of the waves in height. For the shortest waves (λ = 1 km) and an altitude of 0.5 km*, the 22° beam sampled approximately 15% of the length of the wave. The 3° beam, used for height localization, provided a vertical resolution of 45 meters at the nominal elevation angle of 45°. To minimize the influence of phenomena outside the main beam, the sidelobes of both antennas were down greater than 30 dB.

*All altitudes in this report are above mean sea level (MS

The platform of the 3° beam radiometer was designed to provide maximum flexibility. The radiometer was mounted on a vertical wheel so that the antenna normally viewed at an elevation angle of 45° when the liquid nitrogen dewar was vertical. The wheel could then be rotated ± 25° from this 45° angle, giving viewing angles from 20° to 70°. These angles intersected the vertical viewing beam at heights from 183 to 1160 meters, covering the expected altitude range of the internal waves. The vertical wheel was, in turn, mounted on a horizontal wheel which could be rotated 360° in azimuth, permitting the radiometer to view at all azimuth angles.

3.2 NELC Equipment

The equipment available at NELC provides a unique facility for remote sensing of the lower atmosphere. It consists of fixed and mobile FM-CW radars, an acoustic sounder array, lidar, microbarograph, balloon sounding capability, and routine surface meterological data at two sites. The equipment is automated (except balloon soundings) so that observations can be made continuously seven days a week, 24 hours a day. This is essential for studying internal waves since their occurrence is not yet predictable. All of the remote sensors have detected wave activity in the lower atmosphere, although the FM-CW radar is the most sensitive and provides detailed structure with a resolution of one meter. For this reason, and because it is sensitive to moisture fluctuations, the FM-CW radar was the primary sensor compared with the microwave radiometers. The equipment has been described elsewhere in numerous articles, Richter (1969) and McAllister (1968) and will not be repeated here. As a quick review, Table II lists some of the equipment parameters and their sensitivity to atmospheric variables.

TABLE II

NELC Equipment Parameters

1. FM-CW radar (3 GHz, 2.6° beamwidth, resolution = 1 meter, high-sensitivity, detects moisture fluctuations at scale size of 5 cm).

2. Acoustic sounder (7° beamwidth, detects temperature fluctuations at scale size of 8 cm).

3. Lidar (sensitive to aerosol distribution).

4. Microbarograph (monitors surface pressure, sensitivity = 0.01 mb, detects passage of gravity waves).

5. Surface meteorological equipment (temperature, pressure, relative humidity, visibility, wind speed and direction).

6. Balloon soundings (temperature and dew point from surface up to 2000 meters).

4. EXPERIMENTAL PLAN

4.1 Site Location

The experimental site was located at NELC on the western side of the Point Loma Peninsula. To use triangulation for height determination of the waves, the radiometers were separated the distance between the bottom and top of the ridge (see Fig. 2). The vertically pointing radiometer was placed near the ridge top (105 meters altitude) close to the FM-CW radar so as to observe a common volume of air. The scanning 3° bw radiometer was placed on the roof of a building (40 meters altitude) at the bottom of the ridge near the ocean. This provided an unobstructed view in all directions for the scanning radiometer and gave a separation between radiometers of 427 meters. Changing the elevation angle of the 3° beam from 20° to 70° varied the intersection of the two beams from just the top of the ridge up to 1160 meters (see Fig. 3). This covered the expected height range of the inversion layer and the associated internal waves.

4.2 Procedure

Both radiometers took data continuously except during calibrations or refilling of the liquid nitrogen dewars. During normal working hours, calibrations were done manually soon after arrival in the morning and again shortly before leaving at night. At night, an automatic timing device initiated calibrations on a preset schedule, originally set for once per hour, but later changed to once every 12 hours.

The small changes in brightness temperature caused by internal waves required high gain settings on the recorders to obtain the desired sensitivity. However, when large changes in sky brightness temperature were occurring (i.e. clouds forming or dissipating), the pens, if not readjusted, would be driven off scale. For daytime operations, only occasional monitoring of the three strip-chart recorders was required to keep the pens on scale. For nighttime operations, the gain of the recorders would be decreased so as to prevent the complete loss of data. The required gain setting varied from night to night, depending on meteorological conditions. It was discovered that dew would form on the antenna lenses if clear skies occurred for several hours after sunset. This caused a large ($T \approx 100°K$) signal increase over a period of several hours, usually driving the recorders off scale.

The primary use of the narrow (3°) beam radiometer was to localize wave activity in height. The inversion height would be found from either an NELC balloon sounding or from the radiosonde at Montgomery Field (MYF) (12 km away). The correlation of the outputs of the two radiometers was examined when the two beams intersected below, at, and above this inversion height. The height of maximum correlation was then assumed to be the height of the source of internal waves (see Section 5.4).

A brief attempt was made to investigate air parcels at the inversion height, primarily their continuity in time and their speed. The narrow beam radiometer was pointed at a specific azimuth and elevation angle so that the narrow beam intersected the inversion base a certain distance upwind of the vertically pointing beam. The time delay between occurrences at the two raditometers depended on the separation between the antenna beams at the inversion height and the wind speed at this height. By changing the azimuth and elevation angle, various time delays between the two radiometers could be introduced. In this way, the continuity of the parcels along the horizontal direction could be determined as well as their speed.

5. EXPERIMENTAL RESULTS

This section presents three examples of internal wave trains which were observed with one or both microwave radiometers simultaneously with the FM-CW radar. The one-to-one correspondence (to within $\pm$ 1 minute) between fluctuations of the passive (radiometer) and active (FM-CW radar) sensors shows that, in these cases, both sensors are detecting the same waves, even though detection is by different mechanisms. Although only a small number of the total waves observed is shown here, the other cases show agreement with the FM-CW radar similar to that detailed by the cases presented below. Additional examples with analysis will be in the final report. Finally, Section 5.4 provides an extensive discussion of height localization of internal waves, including the principles involved and several examples illustrating different types of behavior.

5.1 Waves on 15 May 1975

On 15 May, when the 3° beam was pointed upwards at 60°, there were correlations of the temperature variations between the radiometer and the waves recorded by the FM-CW radar (Fig. 4). The waves recorded by the FM-CW radar, as shown in Fig. 4, are not large, approximately 18 m in peak-to-peak amplitude for the largest ones, which were at an altitude of 875 meters. The intersection of the two radiometer beams, at a height from 530 to 1260 meters, included the altitude of the waves recorded by the FM-CW radar. The times of the wave crests on the FM-CW record are marked on Fig. 4 and tabulated in Table III. The times of the temperature peaks on the simultaneous 3° beam radiometer trace are marked on Fig. 5 and (also) tabulated in Table III for comparison.

TABLE III

Time of Undulations for Wave Activity on
15 May 1975, (1400-1440 PST), 3° Radiometer, θ = 60°

FM-CW FILM		RADIOMETER	
Crest	Trough	Crest	Trough
1401		1401	
	1407		1406.5
1415		1415	
	1418		1418
1420(S)		1420	
	1421		1421
1422(S)		1422	
	1423		1423.5
1425		1426	
	1428		1428
1430		1430.5	
	1435		1434

(S) small amplitude

The agreement between both the crests and the troughs is within one minute for the six waves. This is within the accuracy of picking crests and troughs without detailed analysis. Further correspondence is found in the time variations of the wave periods; the wave train begins with long period waves, then the periods become shorter and finally become long again.

5.2 Waves on 17 May 1975

The waves observed on 17 May had longer periods (6-10 minutes) than the waves on 15 May. The FM-CW film in Fig. 6 shows the waves outlined by insects (dot echoes), with only intermittent solid outlines. Insects have been used as tracers of atmospheric motion previously (Richter, et al., 1973; Atlas, et al., 1970b), but their appearance during daylight hours (1200 PST) is unusual. In this case, the waves were large, being approximately 90 m peak-to-peak at an altitude of 965 meters. Unfortunately, in this case, the 3° beam radiometer was inoperative during 60% of the wave train, but there is good correlation between the temperature variations on the 22° beam radiometer and the FM-CW radar record. The times of the undulations for both the FM-CW radar (Fig. 6) and the 22° beam radiometer (Fig. 7) are marked and tabulated in Table IV.

TABLE IV

Time of Undulations for Wave Activity on
17 May 1975 (1200-1245 PST), 22° Vertical Radiometer

FM-CW FILM		22° RADIOMETER	
Crest	Trough	Crest	Trough
1208		1208	
	1213		1213
1216.5		1217	
	1219		1219
1223		1223	
	1228		1228
1233		1233	
	1236		1236
1239		1238	
	1242		1243

The agreement between both the wave crests and troughs is again within one minute, even though the wave periods vary from 6 to 10 minutes. In addition to the wave train described above, the radiometer record suggests wave activity between 1300 and 1400 PST which is not shown on the FM-CW record.

5.3 Waves on 23 June 1975

The strongest wave activity occurred during a 1.5-hour period when the 3° beam was pointed upwards at 50° on an azimuth 74° to the south of the vertically viewing radiometer. The FM-CW radar record is shown in Fig. 8 and the corresponding signal for both radiometers is shown in Fig. 9. The FM-CW record shows a large upward change at 0332 PST, a small peak at 0339 PST, followed by a gradual increase until 0400 PST. From this time onward, a series of seven waves starts at 0400 PST and lasts until 0456 PST. The amplitude of the waves is not large, being approximately 30 meters peak-to-peak at an altitude of 600 meters. The base of the inversion is at 660 meters as shown in an NELC balloon sounding taken 2.5 hours later (Fig. 10). This difference in height is not considered significant considering the 2.5-hour time difference, and it can be assumed that the wave activity is occurring near the base of the inversion. In Table V, the times of the waves are listed for both the FM-CW radar and the radiometer.

TABLE V

Time of Undulations for Wave Activity on
23 June 1975 (0330-0500 PST)
3° Radiometer, θ = 50°

FM-CW FILM		RADIOMETERS	
Crests	Troughs	Crests	Troughs
0332		0332	
0339		0339	
0400		0401	
	0405		0406
0409		0409	
	0413		0412
0416		0417	
	0421		0421
0424		0425	
	0429		0430
0432		0434	
	0436		0438
0440		0440	
	0444		0444
0447		0449	
	0452		0453
0456		0457	

The agreement is within a minute for most of the features occurring during the 1.5 hour period. The reason for the large change at 0332 PST on both the FM-CW radar and radiometer signals, some 28 minutes before the wave train occurs, is unknown. It may or may not be connected with the initiation of the internal waves. Further analysis may help answer this and other questions.

5.4 Height Localization

5.4.1 Principles

The model and assumptions, on which height localization is based, are as follows. It is assumed that an internal wave in the inversion layer changes the height of the moist air column above the vertically looking (22° bw) radiometer, and hence the radiometer output. The height change is the amplitude of the wave. In the following procedure, first assume that the narrow (3°) beam intersects the vertical beam (Fig. 3) at the inversion height. The change in column height (included within the 3° beam) times the appropriate geometrical factors, causes the signal change in the 3° beam. The signal outputs of the two radiometers would be correlated with zero lag.

Second, imagine the 3° beam elevated to intersect above the inversion; the waves in the inversion will pass through the 3° beam first, if coming from the west (from the direction of the 3° beam radiometer). If the further assumption is made that the wave train is "frozen" in its propagation direction for the radiometer separation (which is small compared to the usual 1- to 10-km wavelengths of gravity waves), then there will be correlation between the radiometer outputs, but with a time lead (τ) of the 3° beam signal. This lead equals the distance between the 3° and 22° beams at the inversion height divided by the component of the wave propagation velocity along the direction of the two radiometers. If the waves are not completely frozen in this time interval, the magnitude of the cross correlation will be less. Thus, in general, the magnitude of the cross correlation should be greatest for beam intersections at the inversion height and should fall off for intersections above (or below) the inversion. In this experiment, only visual correlation estimates could be made. An electronic correlator will be used in the follow-on experiment.

Third, consider the 3° beam elevated to intersect the vertical 22° beam below the inversion height. The situation will be just the opposite to the previous case, and now there will be a time lag (τ) of the cross correlation function.

Three examples on three different days will be given to show different types of behavior.

5.4.2 Results of 15 May 1975

Table VI summarizes the results of the three data runs on this overcast day.

TABLE VI

15 May 1975
Height Localization Runs

TIME PST	θ 3° Beam Elev. Angle Degree	Beam Intersection Height m	Inversion Height m	Visual Correlation of two radiometer signals	FM-CW
1340-1440	60°	840 (1260 to 590)	945	Good (T > 3 Min)	Excellent correlation of waves at 875 m.
0950-1250	50°	590	900	weak	
1503-1735	30°	285	945	Weak	

Notes: Overcast. Cloud base at 700 to 760 m. Maximum height recordable on acoustic sounder film was approximately 790 m.

The bottom two lines show only weak correlation with the beam intersections considerably below the 945-m inversion height. There is good correlation for periods as short as three minutes at θ = [illegible], where the beam intersection includes both the inversion height (945 m) and the FM-CW wave train height (875 m). In addition, there is excellent correlation of the 3° beam signal peaks and the FM-CW wave crests as shown in Figs. 4 and 5 and Table III.

The data runs therefore localize the wave activity at or above the inversion height. Data runs could not be made with intersection regions completely above the 945-m inversion. It is unlikely however, that any wave activity in the much drier air above the inversion would have more than a minor effect on the radiometers. The rapid decrease in the correlation below the inversion, then implies a similar behavior for intersections above the inversion. It thus seems reasonable that the wave activity has been localized at the inversion height.

5.4.3 Results of 29 June 1975

The summary in Table VII of the data on this clear day shows that there was no correlation between the two radiometer signals for beam intersections either considerably below (195 m) or above (855 m) the 457-m inversion.

TABLE VII

29 June 1975
Height Localization Runs

TIME PST	3° Beam Elev. Angle Degree	Beam Intersection Height m	Inversion Height m	Visual Correlation of two radiometer signals	Acoustic Sounder
0400-0823	32°	310	457 (MYF)	Fair (T > 10 min.)	No return at 305 or 457 m.
0932	45°	470		Very Weak (T > 10 min.)	Irregular return at 457 m.
1052	62°	855		None	
1406	20°	195		Negligible	
1600			427 (MYF)		

Notes: Clear sky. Soundings from Montgomery Field (MYF) used because no soundings at NELC on 29 June. FM-CW film not available at this time.

The two runs at 0823 PST and 0932 PST, with intersections near (310 m) and at the inversion height, show small correlation, but for trends over 10 minutes. At 0823 PST no echoes were obtained by the acoustic sounder from the 305 m or 457 m levels; at 0932 PST the acoustic sounder showed only an irregular return at 457 m but no waves. Since the two runs were made under different conditions, the difference in the correlation magnitude between these two runs is not significant. This lack of wave activity may have contributed to the small correlation; there were not the usual 3- to 5-minute period waves which can be easily correlated visually. The data runs do provide at least the appropriate trends of the localization process, i.e., small correlations for beam

intersections far below or above the inversion, and larger correlations for the two intersections nearer the inversion.

5.4.4 Results of 8 May 1975

The data of the clear day of 8 May 1975 will help to illustrate the additional aid in height localization provided by the time delay (τ) for a maximum magnitude of the cross-correlation function (vs τ) of the signals of the two radiometers.

Table VIII lists the conditions for one 8 May 1975 data run with the 3° beam elevated at 69° and pointed towards the 22° beam to intersect at a height of 1170 m, or above the inversion height of 427m. Good correlation of wave-like activity between the radiometers occurred from 0802 PST to 0825 PST with τ = +2.5 minutes, i.e., the events were 2.5 minutes earlier in the 3° beam signal.

TABLE VIII

8 May 1975
0800 PST Height Localization Run

TIME PST	3° Beam Elev. Angle Degree	Beam Intersection Height m	Inversion Height m	Visual correlation of two radiometer signals	FM-CW
0802-0825	69°	1170 >1830 to 760	457	Good (T > 3 min.) τ = +2.5 min.	Irregular trace no waves. (See text). Height of 523 m.
0825-0838				None	
0853-0908				None	
0918-0938				None	
0953-1011				Some (T > 10 min.)	
1103-1138				Some (T > 10 min.)	

Notes: Sky changed from overcast (610 m) to clear at 0800 PST.
Winds - MVF 0400 PST sounding.

Altitude	Direction Degree	Speed $msec^{-1}$
305	-	0
610	310	0.5
915	345	1.0
1220	005	1.5

For the second data run on 8 May 1975, the 3° beam was elevated 25° to intersect the 22° beam at height of 240 m, or below the 427-m inversion. The data and conditions are listed in Table IX. During the time 1252 to 1318 PST, there was "medium" correlation of the 4.5-minute period variations of the two radiometer signals, with those of the 3° beam being delayed 1.3 minutes, instead of being earlier as they were at $\theta = 69°$. Near this time, at 1400 PST, there were five wave crests on the FM-CW radar film at a height of 442 m which correclated with the 3° beam radiometer signal peaks, the radiometer peaks being an average of 1.5 minutes later (Table IX). The FM-CW film, in this case, served to verify the delay obtained from the cross correlation between the two radiometer signals.

TABLE IX

8 May 1975

A. 1400 PST Height Localization Run
Clear sky

TIME PST	θ 3° Beam Elev. Angle Deg.	Beam Inter-section Height m	Inversion Height m	Visual correlation of two radiometer Signals	FM-CW
1140			427		
1252-1318	25°	240		Medium (T > 3 min.) τ =-1.3 min.	
1400-1419	25°	240			Good correlation of waves at 442m.

B. Correlation of FM-CW Waves and 3° bw Radiometer Waves: 20 to 30 meter amplitude at 442 -m altitude

Time of FM-CW Crests PST	Time of 3°bw radiometer peaks PST	Difference Minutes
1400	1401	1.0
1403.5	1405	1.5
1408	1409	1.0
1412	1413.5	1.5
1416	1418.5	2.5

Average difference = τ = -1.5 min.
(3° beam later).

C. Winds - MYF 1600 PST 8 May 1975 Sounding

Altitude	Direction Deg.	Speed m sec^{-1}
305	250	3.5
610	210	1.0
915	175	2.0
1220	170	3.5

The use of the time shifts for height localization requires that the wave activity propagate through the two beams at constant altitude, speed, and direction. For example, if one postulates that the same wave activity moving through the two beams produced the 2.5-minute lead at $\theta = 69°$ and a 1.3-minute lag at $\theta = 25°$, an examination of Fig. 3 shows that waves at an altitude of 300 m, coming from the west, could account for such time shifts. However, since conditions had changed in the six hour interval between the two data runs, an accurate calculation cannot be made for this particular data run, but the procedure is illustrated.

The data illustrates a case of noncorrespondence between the radiometer and the FM-CW radar. At 0800 PST, the inversion base was at 457 m, but the activity on the FM-CW radar film was at 523 m. Although correlation was established at 1400 PST between the FM-CW waves and the radiometer signal, no such correlation could be found at 0800 PST. In fact, the 0802-0825 PST period on the FM-CW film was broken up as follows:

0802-0813 PST: an irregular trace - no recognizable wave train.
0813-0820 PST: the trace disappears.
0820-0822 PST: trace reappears.
0822-0830 PST: trace disappears.

These two differences, coupled with the fact that the inversion base altitude remained nearly constant during the six hours (457 m to 427 m), make it uncertain (and even unlikely) that the FM-CW film trace at 523 m is what the radiometer is observing at 0800 PST. Further evidence lies in the winds (see Table VIII) of only 0.5 m sec^{-1} at 610 m and zero at 305 m; the shear is far below the 0.01 sec^{-1} value set by Atlas (1970) to produce turbulence. This lack of turbulence is probably why the activity at the 457-m inversion height is not seen on the FM-CW film. Therefore, it is reasonable to assume that wave activity at the 457-m inversion height is what propagated through the two radiometer beams at 0800 PST and produced the cross-correlation of the two beams.

6. CONCLUSIONS

Two series of radiometric measurements at the 22.2 GHz-water vapor line were made during May and June 1975. Results of preliminary analysis show both detection of internal waves in the lower atmosphere and their localization in height. Correspondence between wave activity as observed by the FM-CW radar and the microwave radiometers exists within $\pm$ 1 minute for several cases considered. The 0.1° to 0.7° K magnitude of brightness temperature changes observed by the radiometer compares to that predicted by an internal wave model of 0.1 to 0.4° K. Further analysis of the data and a follow-on experiment are now in progress to determine the mechanism responsible for the detection of internal waves with microwave radiometers and to evaluate the possibility of using ground-based microwave radiometers as remote sensors of refractive index variations.

7. ACKNOWLEDGEMENTS

The authors wish to express their special appreciation for the invaluable assistance of G. Hermann in supervising the design, construction, and operation of the instrumentation used in this experiment. In addition, the authors appreciate the help and cooperation of B. Au for radiometer design, J. Kenney for circuitry, and F. Sollner and B. Kremer for construction and field installation. Finally, we wish to express our appreciation to the NELC personnel for their cooperation and assistance during this measurement program.

8. REFERENCES

Atlas, D., J.I. Metcalf, J.H. Richter, and E.E. Gossard, "The Birth of "Cat" and Microscale Turbulence," J. Atmos. Sci., 27, 903-913, 1970a

Atlas, D., F.I. Harris and J.H. Richter, "Measurement of Point Target Speeds with Incoherent Non-Tracking Radar: Insect Speeds in Atmospheric Waves," J. Geophys. Res., 75, 7588-7595, 1970b

Gossard, E.E. and W.H. Munk, "On Gravity Waves in the Atmosphere," J. Meteor., 11, 259-269, 1954

Gossard, E.E., J.H. Richter and D. Atlas, "Internal Waves in the Atmosphere from High Resolution Radar Measurements," J. Geophys. Res., 75, 3532-3536, 1970

Gossard, E.E., D.R. Jensen and J.H. Richter, "Analytical Study of Tropospheric Structure as Seen by High-Resolution Radar," J. Atmos. Sci., 28, 794-807, 1971

Gossard, E.E. and Hooke, W.H., Waves in the Atmosphere, Elsevier Scientific Publishing Co., Amsterdam, 1975.

Kreiss, W.T., "Meteorological Observations with Passive Microwave Systems," The Boeing Company, Seattle, Washington, 98124. Tech Rept. DI-82-0692, February 1968

McAllister, L.G., "Acoustic Sounding of the Lower Troposhere," J. Atmospheric Terrest. Phys. 30, 1439-1440, 1968

Richter, J.H., "High Resolution Tropospheric Radar Sounding," Radio Science, 4, 1261-1268, 1969

Richter, J.H., D.R. Jensen, W.F. Noonkester, J.B. Preaskey, R.A. Stinmann and W.W. Wolf, "Remote Radar Sensing: Atmospheric Structure and Insects," Science, 180, 1176-1178, 1973

Vickers, W.W. and M.E. Lopez, "Low-angle radar tracking errors induced by non stratified atmospheric anomalies," Radio Science, 10, 491-505, 1975.

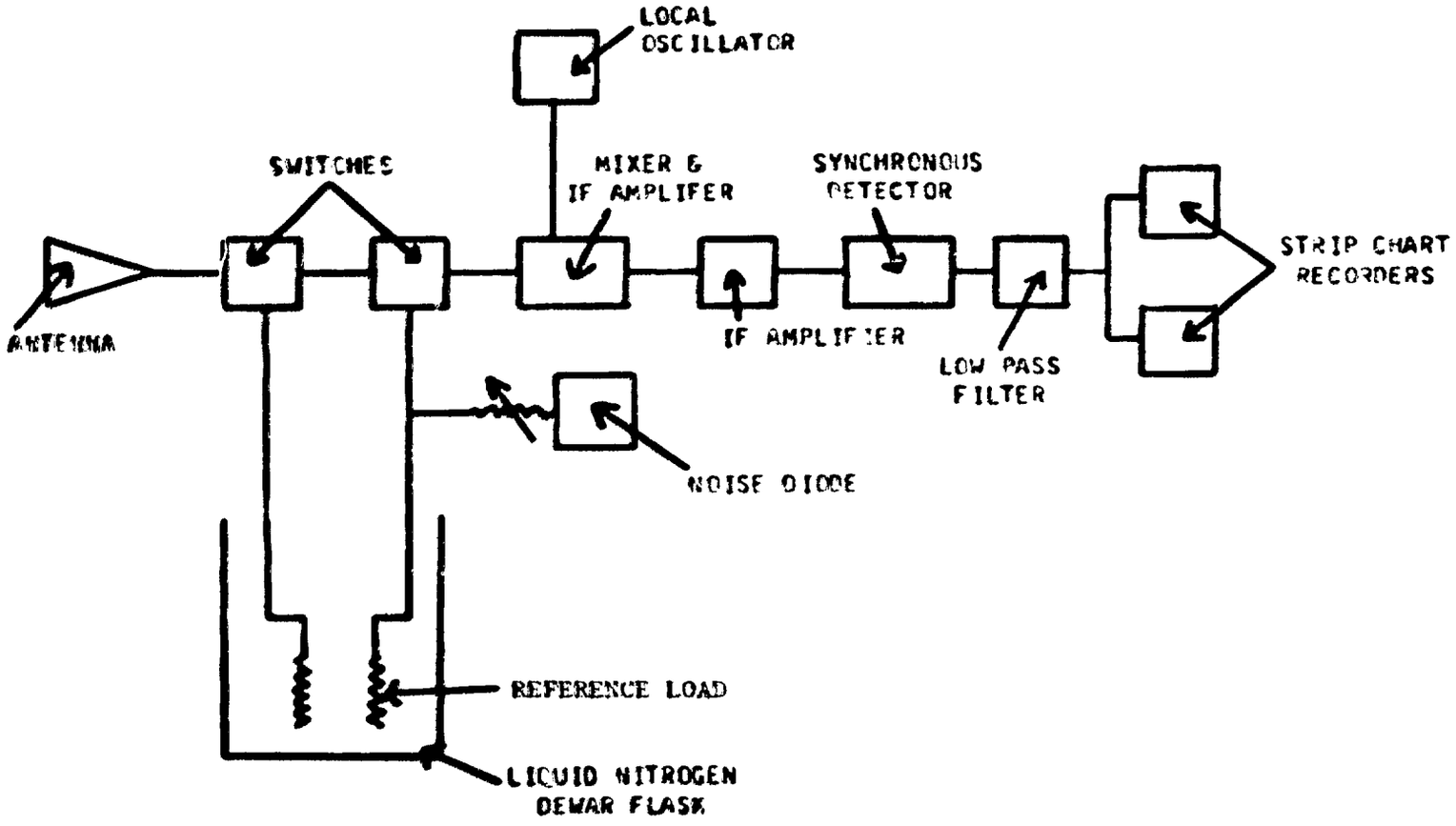

Fig. 1 — Block diagram of Dicke radiometer used in wave experiment

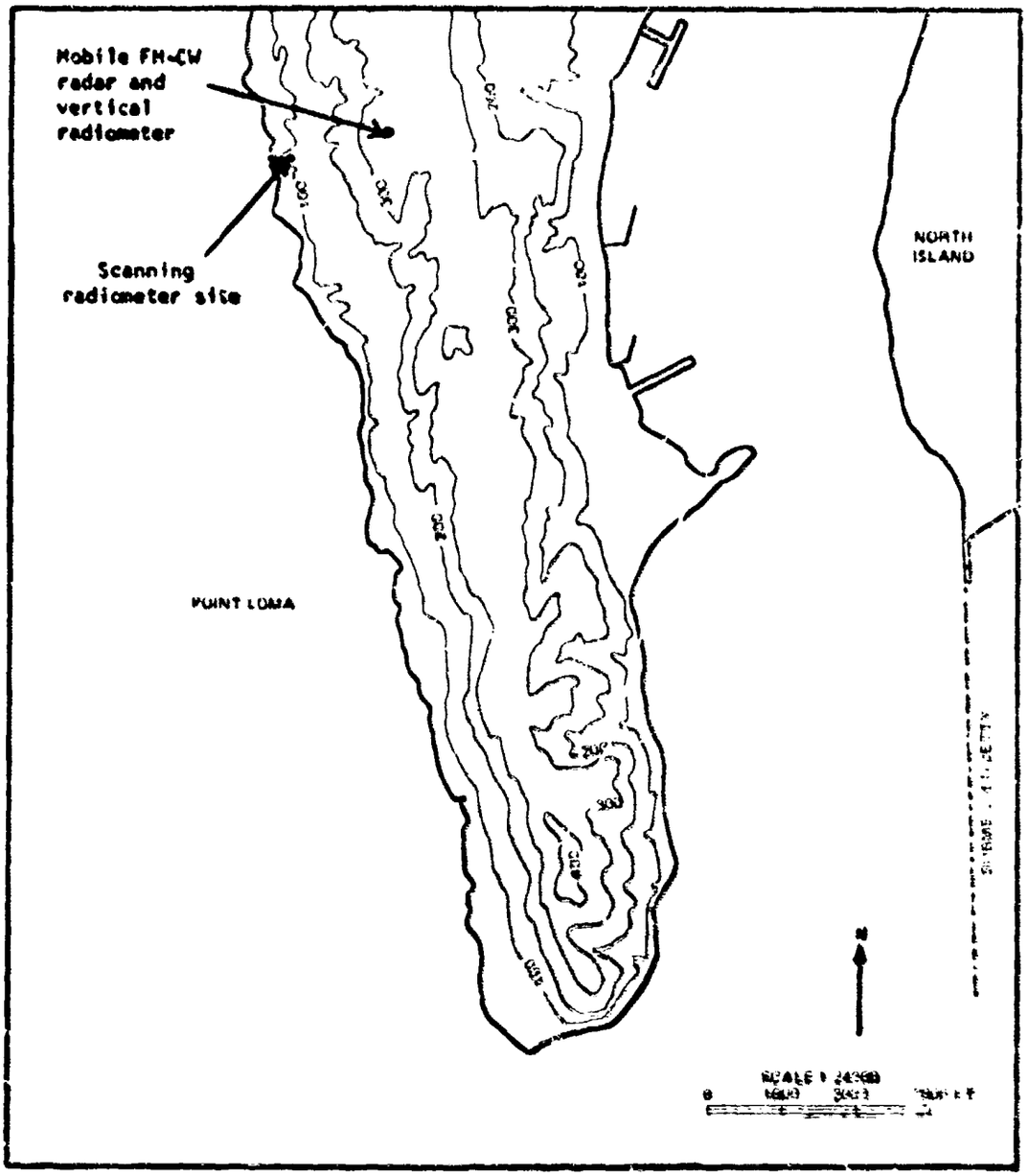

Fig. 2 – Topographic map of southern Point Loma Peninsula where the internal wave experiment was located. (Height contours in feet.)

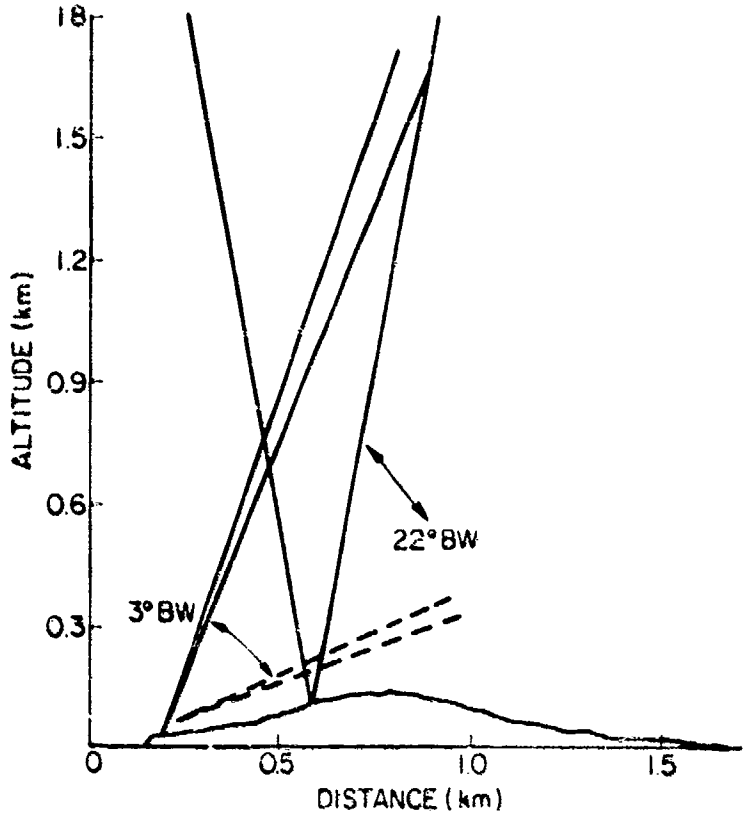

Fig. 3 — Cross-section of Point Loma Peninsula, San Diego, California showing location of wide (22°) and narrow (3°) beamwidth 22 GHz radiometers for detection of internal waves

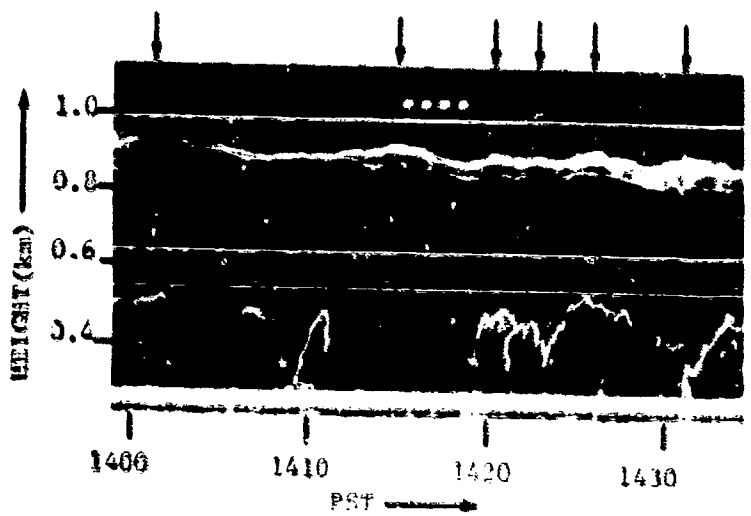

Fig. 4 — Intensity-modulated, height-time FM-CW radar record of 15 May 1975, 1400-1435 PST. Internal waves (crests denoted by arrows) appear at an altitude of 875 meters. Intermittent echoes below 550 meters are due to buoyant elements rising from the surface.

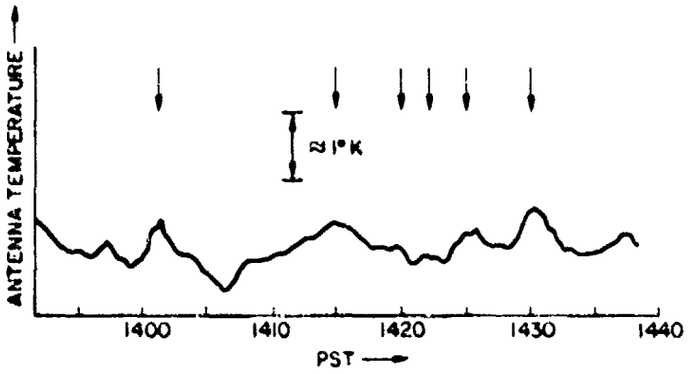

Fig. 5 — Signal of 3° bw microwave radiometer versus time for 15 May 1975, 1400-1440 PST. Times of internal wave crests are denoted by arrows at the top of the figure. Elevation angle = 60°, azimuth angle = 76°.

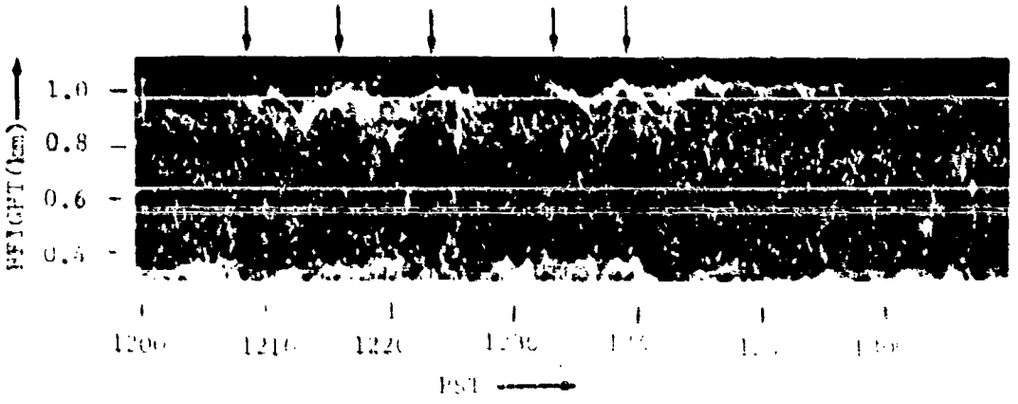

Fig. 6 — Intensity-modulated, height-time FM-CW radar record of 17 May 1975, 1200-1300 PST. Internal waves (crests denoted by arrows) are outlined by dot echoes from insects at altitude of 965 meters. Echoes below 300 meters are due to returns from convective cells.

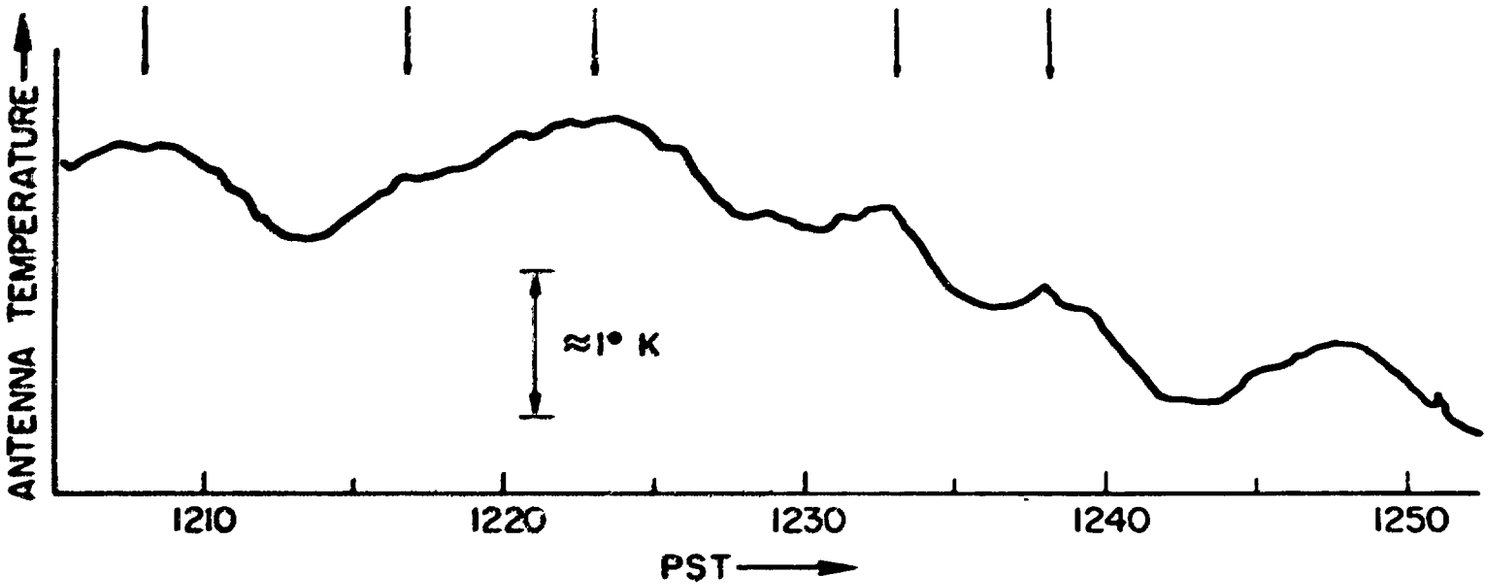

Fig. 7 — Signal of 22° bw microwave radiometer versus time for 17 May 1975, 1210-1250 PST. Times of internal wave crests are denoted by arrows at the top of the figure.

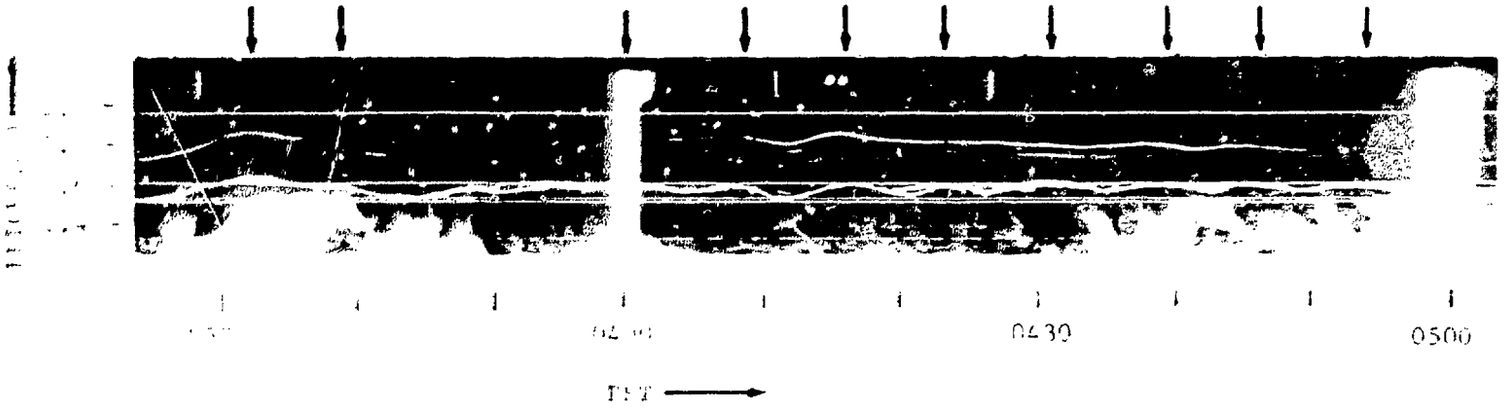

Fig. 8 — Intensity-modulated, height-time FM-CW radar record of 23 June 1975, 0320-0450 PST. Internal waves (crests denoted by arrows) appear at an altitude of 600 meters and have been outlined for clear photographic reproduction. Waves are also induced in the dry air above at 843 meters. Light regions below 550 meters are due to radar return from drizzle.

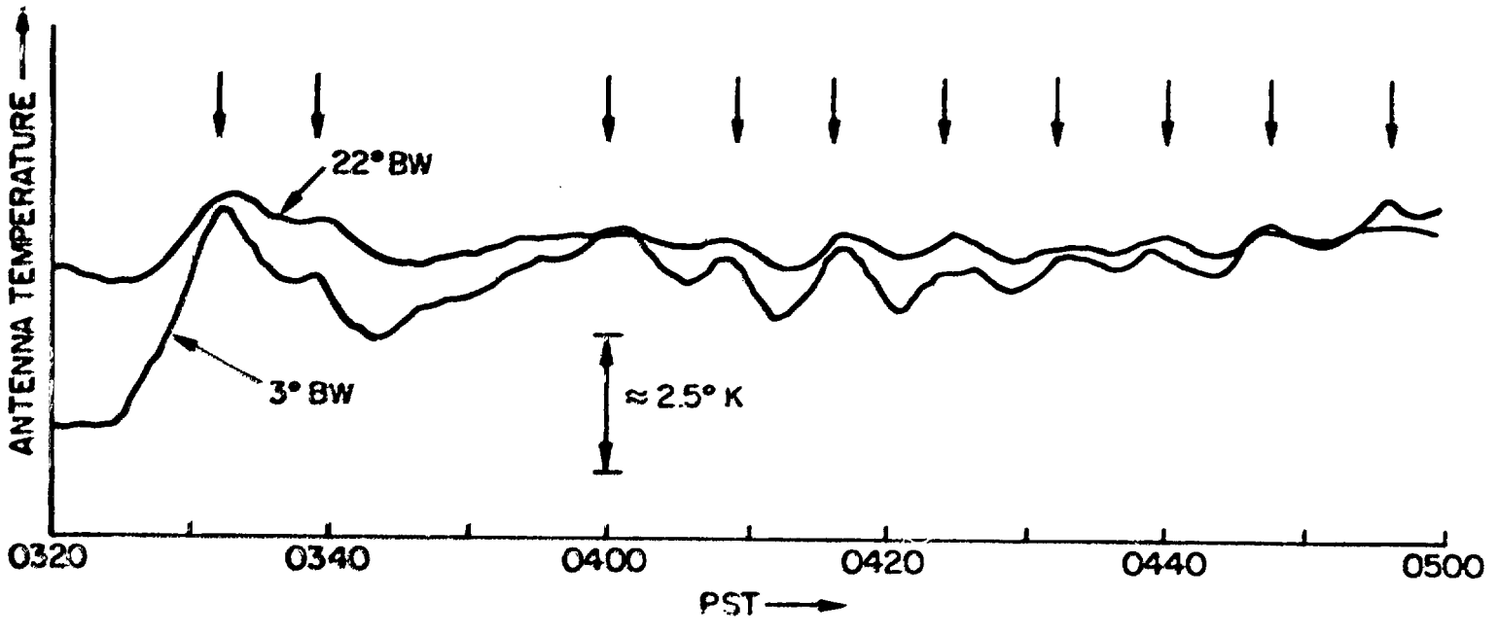

Fig. 9 — Signals of 3° and 22° bw microwave radiometers versus time for 23 June 1975, 0320-0500 PST. Times of internal wave crests are denoted by arrows at top of figure. Elevation angle = 50°, azimuth angle = 150°.

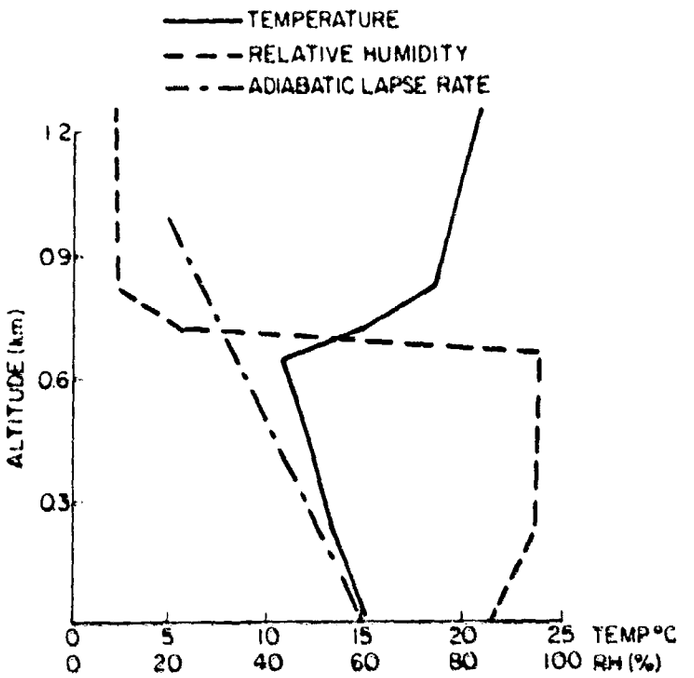

Fig. 10 — Temperature and relative humidity height profiles from NELC radiosonde on 23 June 1975, 0730 PST